International Journal of Innovative Research and Scientific Studies, 8(7) 2025, pages: 405-417

IJIRSS
International Journal of Innovative Research & Scientific Studies

ISSN: 2617-6548

URL: www.ijirss.com

Analysis of temperature increase impact on oxygen depletion

RS Lebelo[1*], MH Langa[2], SO Adesanya[3,4], NL Kaeane[4]

[1]*Vaal University of Technology, Faculty of Applied and Computer Science, Vanderbijlpark, South Africa.*
[2]*Vaal University of Technology, Faculty of Engineering and Technology, Vanderbijlpark, South Africa.*
[3]*Redeemer's University, Faculty of Natural Sciences, Ede 232101, Osun State, Nigeria.*
[4]*Vaal University of Technology, Faculty of Human Science, Vanderbijlpark, South Africa.*

Corresponding author: RS Lebelo (*Email: sollyl@vut.ac.za*)

Abstract

One of the significant challenges in urbanization and industrialization is the release of harmful reactive contaminants that undergo exothermic chemical reactions into drinking water sources. This challenge is of interest even to the United Nations in ensuring clean water, environments free of hazardous material, and good health. In this article, a mathematical examination of the heat generation due to exothermic chemical reaction in water is conducted on the dissolved oxygen level for aquatic life and the emergence of dangerous bacteria and algae that could trigger water-related diseases. The study compares the temperature rise in a one-step (includes one activation energy profile), two-step (includes two activation energy profiles), and three-step (includes three activation energy profiles) exothermic chemical reactions to observe how the oxygen depletion rate occurs accordingly. The appropriate equations governing the heat and mass transfer within the cylindrical channel are formulated, presented in dimensionless form, and solved numerically using the Runge-Kutta Fehlberg method in conjunction with the Shooting technique. The results indicate that the oxygen depletion in a one-step exothermic chemical reaction is less than in the two-step reaction and is highest in the three-step condition, as the temperature increase strength is observed from one-step to three-step situation. Moreover, the results show that the temperature intensity becomes stronger as the reaction mechanism steps increase from one to three.

Keywords: Exothermic chemical reaction, Numerical methods, Oxygen depletion, Runge-Kutta Fehlberg method, Shooting technique. Temperature rise.

DOI: 10.53894/ijirss.v8i7.10457
Funding: This study received no specific financial support.
History: Received: 7 August 2025 / **Revised:** 9 September 2025 / **Accepted:** 12 September 2025 / **Published:** 2 October 2025

Competing Interests: The authors declare that they have no competing interests.
Authors' Contributions: All authors contributed equally to the conception and design of the study. All authors have read and agreed to the published version of the manuscript.
Transparency: The authors confirm that the manuscript is an honest, accurate, and transparent account of the study; that no vital features of the study have been omitted; and that any discrepancies from the study as planned have been explained. This study followed all ethical practices during writing.
Acknowledgement: The acknowledge the Vaal University of Technology for availing facilities to produce this work.
Publisher: Innovative Research Publishing

1. Introduction

In the last few years, there has been increased attention on studies of thermal effect on water bodies due to industrialization. The impact of exothermic reactive contaminants that deplete the oxygen level and raise the water temperature to encourage the growth of harmful microbes in drinking water sources is of interest. It is a known factor that a temperature rise in an exothermic chemical reaction results in oxygen depletion. To emphasize this concept, several researchers investigated the effect of temperature elevations in oceans, rivers, lakes, and pools on the depletion of dissolved oxygen (DO). The purpose of this study is to demonstrate the rate of temperature increase in water that results in oxygen depletion within the water. Water without enough oxygen causes living species within it to die, which contributes to water contamination.

Given these challenges, Mahaffey, et al. [1] elaborated on the importance of oxygen for the respiration of marine bacteria, animals, plants, and other species that live in water. They explained further that DO concentration has been reduced by 2% since 1960. Global warming has also contributed to temperature increases in the past 50 years in coastal seas, and fauna in aquatic environments can experience varied stresses due to water temperatures increasing, and it is also expected that this scenario can exist for the coming 100 years [2, 3]. In deep water ecosystems, DO integrates chemical, physical, and biological processes such as photosynthesis, respiration, and organic matter decomposition, and therefore affects issues related to human-derived services of the ecosystem, including the quality of fresh water and provision of food [3]. Furthermore, Rajwa-Kuligiewicz, et al. [4] confirm that DO also plays a role in indicating rivers' biological health, especially those exhibiting fluctuations of spatial and temporal scales. Roman, et al. [5] claim that DO in coastal waters is also caused by human activities such as agriculture, changes in land usage, and loading of point-source nutrients. They also mentioned that low DO in coastal systems causes fish and zooplankton not to develop specific physiological adaptations. Moreover, Lewis, et al. [6] claim that the decline in DO in freshwater and marine ecosystems causes an unfavorable aquatic habitat for various organisms. It is noted that the water quality in lakes also depends on DO and that a decrease in its content is detrimental to the lake's ecosystem; furthermore, an increase in the lake's temperature decreases the DO concentration [7-9]. It is also ascertained in Rajesh and Rehana [10] and Chapra, et al. [11] that the river water temperature (RWT) and Dissolved Oxygen (DO) are both signals for the health definition of the body of river water ecosystems. The relationship between temperature and oxygen is elaborated in BOQU [12] applying Henry's law, stating that "the solubility of oxygen decreases as temperature increases." This means warm water cannot sustain DO, which may lead to oxygen stress in aquatic organisms and deter normal metabolism and growth rates. The fish population can be reduced due to decreased DO.

In a recent study, Oschlies, et al. [13] explained that oxygen reduction in water contributes to lethal or sublethal impacts on humans and the ecosystem. In addition, this shortage of oxygen negatively impacts the reproduction, growth, behaviors, vision, and distribution of species. Motivated by the study in Oschlies, et al. [13] this study aims to investigate the impact of reactive contaminants on the oxygen depletion rate in an exothermic chemical reaction. The mathematical approach to this study offers an understanding of temperature increase and oxygen depletion processes in a quicker manner as compared to the expensive experimental approach. The resulting mathematical model is strongly nonlinear due to the three-step reactions that strictly follow Arrhenius kinetics and do not have exact solutions. As a result, a numerical solution will be obtained based on the combination of the shooting method and the Runge-Kutta approach. This study uses a theoretical approach to studying how temperature increases as the reaction mechanisms step increases from one step to the next, how the oxygen depletion likewise increases, to give a better understanding of how the dissolved oxygen depletion occurs with increased temperature in waters. The gap this study brings is the introduction of the three-step exothermic reaction and the demonstration of heat transfer intensity from one-step through to three-step conditions. The literature available studied heat transfer and reactant consumption in one-step and two-step scenarios only, and this study extends the process to the three-step scenario. The literature survey reveals the novelty of the work since the mathematical analysis reported here has not been conducted as far as we know. The following section will present the theoretical framework on which the model is built and the modelling assumptions.

2. Mathematical Formulation

A one-dimensional irreversible reaction mechanism is assumed to investigate the temperature increase and oxygen depletion in different steps of exothermic chemical reactions. The problem is modeled in a cylindrical domain, and a steady-state reaction mechanism for the energy and mass transfer equations is considered with radiative heat loss to the environment. Heat loss through radiation is represented by Stefan-Boltzmann's law, $q = \mu\sigma(T^4 - T_w^4)$, where μ represents the cylinder's emissivity, and σ the constant for Stefan-Boltzmann. Figure 1 below shows the geometry of the problem.

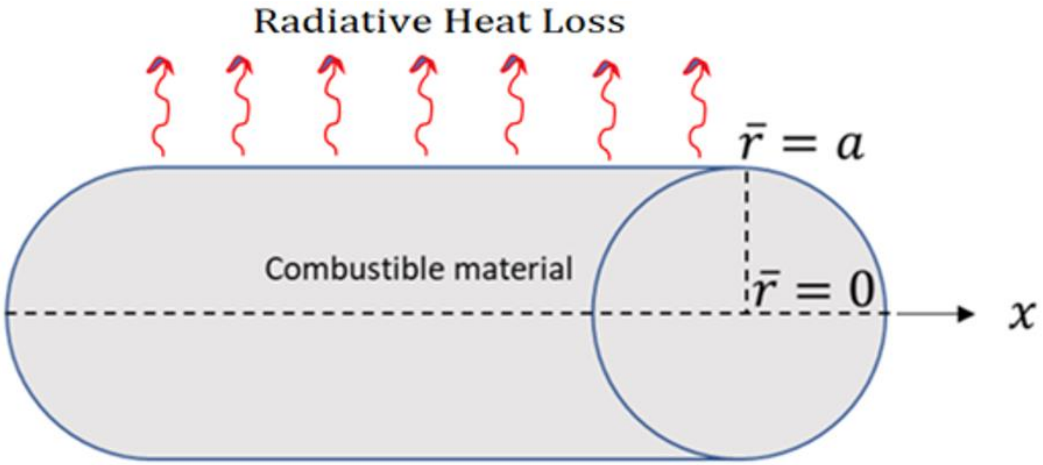

Figure 1.
Geometry of the problem.
Source: Lebelo, et al. [14].

Equations 1 – 2 represent the one-step and two-step exothermic chemical reactions for the coupled temperature and oxygen depletion [15-17].

$$\left.\begin{aligned} \frac{k}{\bar{r}}\frac{d}{d\bar{r}}\left(\bar{r}\frac{dT}{d\bar{r}}\right) + Q_1A_1C_1\left(\frac{KT}{vl}\right)^m e^{-E_1/RT} - \mu\sigma(T^4 - T_w^4) = 0 \\ D\frac{k}{\bar{r}}\frac{d}{d\bar{r}}\left(\bar{r}\frac{dC}{d\bar{r}}\right) - A_1C_1\left(\frac{KT}{vl}\right)^m e^{-E_1/RT} = 0 \end{aligned}\right\} \quad (1)$$

$$\left.\begin{aligned} \frac{k}{\bar{r}}\frac{d}{d\bar{r}}\left(\bar{r}\frac{dT}{dr}\right) + Q_1A_1C_1\left(\frac{KT}{vl}\right)^m e^{-E_1/RT} + Q_2A_2C_2\left(\frac{KT}{vl}\right)^m e^{-E_2/RT} - \mu\sigma(T^4 - T_w^4) = 0 \\ D\frac{k}{\bar{r}}\frac{d}{d\bar{r}}\left(\bar{r}\frac{dC}{d\bar{r}}\right) - A_1C_1\left(\frac{KT}{vl}\right)^m e^{-E_1/RT} - A_2C_2\left(\frac{KT}{vl}\right)^m e^{-E_2/RT} = 0 \end{aligned}\right\} \quad (2)$$

Equation 3 represents a three-step process for an exothermic chemical reaction.

$$\left.\begin{aligned} \frac{k}{\bar{r}}\frac{d}{d\bar{r}}\left(\bar{r}\frac{dT}{d\bar{r}}\right) + Q_1A_1C_1\left(\frac{KT}{vl}\right)^m e^{-E_1/RT} + Q_2A_2C_2\left(\frac{KT}{vl}\right)^m e^{-E_2/RT} + \\ +Q_3A_3C_3\left(\frac{KT}{vl}\right)^m e^{-E_3/RT} - \mu\sigma(T^4 - T_w^4) = 0 \\ D\frac{k}{\bar{r}}\frac{d}{d\bar{r}}\left(\bar{r}\frac{dC}{d\bar{r}}\right) - A_1C_1\left(\frac{KT}{vl}\right)^m e^{-E_1/RT} - A_2C_2\left(\frac{KT}{vl}\right)^m e^{-E_2/RT} - A_3C_3\left(\frac{KT}{vl}\right)^m e^{-E_3/RT} = 0 \end{aligned}\right\} \quad (3)$$

The boundary conditions are as follows.

$$\frac{dT}{d\bar{r}}(0) = 0;\ T(a) = T_w;\ C(0) = C_w;\ C(a) = C_w. \quad (4)$$

Here, $R, C_w, D,$ are the universal gas constant, oxygen concentration on the cylinder's surface, and oxygen diffusivity in the cylinder. The Planck number, vibration frequency, Boltzmann constant, are represented by l, v, K. The m represents the chemical reaction kinetics type, where $m = -2$ is the sensitized, $m = 0$ the Arrhenius and $m = 0.5$ the bimolecular kinetics, with $\bar{r}$ the radial length. In addition, k is the material's thermal conductivity, Q_1, A_1 are the first step's heat of reaction, and rate constant, Q_2, A_2 are for the heat of reaction, and rate constant for the second step, with, Q_3, A_3 the heat of reaction, and the rate constant for the third step. E_1, E_2 and E_3 are the respective activation energy for the first, second, and third steps. It should be noted further that T represents the material's absolute temperature, and T_w the ambient temperature. C_1, C_2, C_3 represent the oxygen concentration for the first, second, and third steps of exothermic chemical reactions.

The nonlinear differential equations are numerically solved by first converting a set of Equations 1 – 4 into nondimensional forms. Nondimensionalization, also called problem normalization is a technique of grouping together, or scaling parameters or variables of the same units to produce physical properties without units [18]. The technique is useful to reduce the complexity and size of differential equations with less parameters that are suitable to solve numerically, as compared to their dimensional expressions [19]. The dimensionless equations are presented as follows:
For Equation 1:

$$\theta_1 = \frac{E_1(T-T_w)}{RT_w^2}, \Phi_1 = \frac{C_1}{C_w}, \epsilon_1 = \frac{kRT_W^2}{Q_1E_1DC_w}\ \ r = \frac{\bar{r}}{a},\quad \varphi_1 = \frac{RT_w}{E_1}, Ra_1 = \frac{\mu\sigma E_1a^2T_w^2}{kR}, \lambda_1 = \left(\frac{KT_w}{vl}\right)^m \frac{Q_1A_1C_1E_1a^2}{kRT_w^2}e^{-E_1/RT}.$$

The non-dimensional form is:

$$\frac{1}{r}\frac{d}{dr}\left(r\frac{d\theta_1}{dr}\right)+\lambda_1(1+\varphi_1\theta_1)^m\Phi_1 e^{\theta_1/(1+\varphi_1\theta_1)}-Ra_1[(\varphi_1\theta_1+1)^4-1]=0.$$
$$\frac{1}{r}\frac{d}{dr}\left(r\frac{d\Phi_1}{dr}\right)-\lambda_1\epsilon_1(1+\varphi_1\theta_1)^m\Phi_1 e^{\theta_1/(1+\varphi_1\theta_1)}=0 \quad (5)$$

For Equation 2:

$$\theta_2=\frac{E_2(T-T_W)}{RT_W^2},\ \Phi_2=\frac{C_2}{C_w},\epsilon_2=\frac{kRT_W^2}{Q_2E_2DC_w},\varphi_2=\frac{RT_W}{E_2},\alpha_1=\frac{E_2}{E_1},\beta_1=\frac{Q_2A_2C_2E_2}{Q_1A_1C_1E_1}e^{(E_1-E_2)/RT},$$
$$Ra_2=\frac{\mu\sigma E_2a^2T_W^2}{kR},\ \lambda_2=\left(\frac{KT_W}{vl}\right)^m\frac{Q_2A_2C_2E_2a^2}{kRT_W^2}e^{-E_2/RT}.$$

The non-dimensional form is:

$$\frac{1}{r}\frac{d}{dr}\left(r\frac{d\theta_2}{dr}\right)+\lambda_2(1+\varphi_2\theta_2)^m\Phi_2\left[e^{\theta_2/(1+\varphi_2\theta_2)}+\beta_1e^{\alpha_1\theta_2/(1+\varphi_2\theta_2)}\right]+$$
$$-Ra_2[(\varphi_2\theta_2+1)^4-1]=0$$
$$\frac{1}{r}\frac{d}{dr}\left(r\frac{d\Phi_2}{dr}\right)-\lambda_2(1+\varphi_2\theta_2)^m\Phi_2\left[\epsilon_2e^{\theta_2/(1+\varphi_2\theta_2)}+e^{\alpha_1\theta_2/(1+\varphi_2\theta_2)}\right]=0 \quad (6)$$

For Equation 3:

$$\theta_3=\frac{E_3(T-T_W)}{RT_W^2},\Phi_3=\frac{C_3}{C_w},\epsilon_3=\frac{kRT_W^2}{Q_3E_3DC_w},\varphi_3=\frac{RT_W}{E_3},\alpha_2=\frac{E_3}{E_2},\beta_2=\frac{Q_3A_3C_3E_3}{Q_2A_2C_2E_2}e^{(E_2-E_3)/RT},$$
$$Ra_3=\frac{\mu\sigma E_3a^2T_W^2}{kR},\ \lambda_3=\left(\frac{KT_w}{vl}\right)^m\frac{Q_3A_3C_3E_3a^2}{kRT_w^2}e^{-E_3/RT}$$

The non-dimensional form is:

$$\frac{1}{r}\frac{d}{dr}\left(r\frac{d\Phi_3}{dr}\right)+\lambda_3(1+\varphi_3\theta_3)^m\Phi_3\left[e^{\theta_3/(1+\varphi_3\theta_3)}+\beta_1e^{\alpha_2\theta_3/(1+\varphi_3\theta_3)}+\beta_2e^{\alpha_2\theta_3/(1+\varphi_3\theta_3)}\right]+$$
$$-Ra_3[(\varphi_3\theta_3+1)^4-1]=0$$
$$\frac{1}{r}\frac{d}{dr}\left(r\frac{d\Phi_3}{dr}\right)-\lambda_3(1+\varphi_3\theta_3)^m\Phi_3\left[\epsilon_3e^{\theta_3/(1+\varphi_3\theta_3)}+e^{\alpha_2\theta_3/(1+\varphi_3\theta_3)}+e^{\alpha_2\theta_3/(1+\varphi_3\theta_3)}\right]=0. \quad (7)$$

The boundary conditions are

$$\frac{d\theta}{dr}(0)=0;\ \theta(1)=0;\ \Phi(0)=1;\ \Phi(1)=1. \quad (8)$$

In this case, $\theta_1,\theta_2,\theta_3$, are the dimensionless temperatures for the respective steps, λ is the Frank-Kamenetskii parameter, also called the reaction rate parameter, $\varphi_1,\varphi_2,\varphi_3$, are the respective dimensionless activation energy parameters for the three steps, r is the dimensionless radial distance, α_1, α_2, are the activation energy ratio parameters for the second and third steps, β_1,β_2 are the exothermic chemical reaction parameters for the second and third steps and Ra_1,Ra_2,Ra_3 are the dimensionless radiation parameters for the three steps. Φ_1,Φ_2,Φ_3 are the dimensionless concentrations and $\epsilon_1,\epsilon_2,\epsilon_3$ are the oxygen consumption rate parameters in respective steps.

2.1. Numerical Solution Approach

The Runge-Kutta Fehlberg (RKF45) method coupled with the Shooting technique was used to solve the nonlinear differential equation for each exothermic chemical reaction step [20]. The RKF45 includes the following steps for the solution [21]:

$$s_2=s_1+\lambda\epsilon_1(1+\varphi z)^me^{z/(1+\varphi z)}$$
$$k_1=\mathrm{h}f(t_i,y_i)$$
$$k_2=\mathrm{h}f(t_i+\tfrac{1}{4}h,y_i+\tfrac{1}{4}k_1)$$
$$k_3=\mathrm{h}f(t_i+\tfrac{3}{8}h,y_i+\tfrac{3}{32}k_1+\tfrac{9}{32}k_2)$$
$$k_4=\mathrm{h}f(t_i+\tfrac{12}{13}h,y_i+\tfrac{1932}{2197}k_1-\tfrac{7200}{2197}k_2+\tfrac{7296}{2197}k_3)$$
$$k_5=\mathrm{h}f(t_i+h,y_i+\tfrac{439}{216}k_1-8k_2+\tfrac{3680}{513}k_3-\tfrac{845}{4104}k_4)$$
$$k_6=\mathrm{h}f(t_i+\tfrac{1}{2}h,y_i-\tfrac{8}{27}k_1+2k_2-\tfrac{3544}{2565}k_3+\tfrac{1859}{4104}k_4-\tfrac{11}{40}k_5)$$

The first approximation of the solution is done by the Runge-Kutta of order 4 given as follows:

$$y_{i+1}=y_i+\tfrac{25}{216}k_1+\tfrac{1408}{2565}k_3+\tfrac{2197}{4104}k_4-\tfrac{1}{5}k_5. \quad (9)$$

The Runge-Kutta method of order 5 is then used for better solution value determination as given by the following equation:

$$z_{i+1}=y_i+\tfrac{16}{135}k_1+\tfrac{6656}{12825}k_3+\tfrac{28561}{56430}k_4-\tfrac{9}{50}k_5+\tfrac{2}{55}k_6. \quad (10)$$

The discreet points set of error control tolerance ϵ are used to compute an IVP numerical approximation at a given interval, [22] The following equation contains error control ϵ:

$$n=0.840896\left(\frac{\epsilon\mathrm{h}}{|z_{i+1}-y_{i+1}|}\right)^{\frac{1}{4}}.$$

Where n, h are respectively the scalar and the step size, with nh being the optimal step size. The expression $\mathrm{E}=z_{i+1}-y_{i+1}$, where E is the error estimate, is also described by the equation:

$$\mathrm{E}=\tfrac{1}{360}k_1-\tfrac{128}{4275}k_3-\tfrac{2197}{75240}k_4+\tfrac{1}{50}k_5+\tfrac{2}{55}k_6. \quad (11)$$

The first part of Equation 5 was used to demonstrate the smoothness of the solution which tends to confirm the stability of the RKF45 and the error minimization. Figure 2 demonstrates the smoothness and convergence of the solution by RKF45.

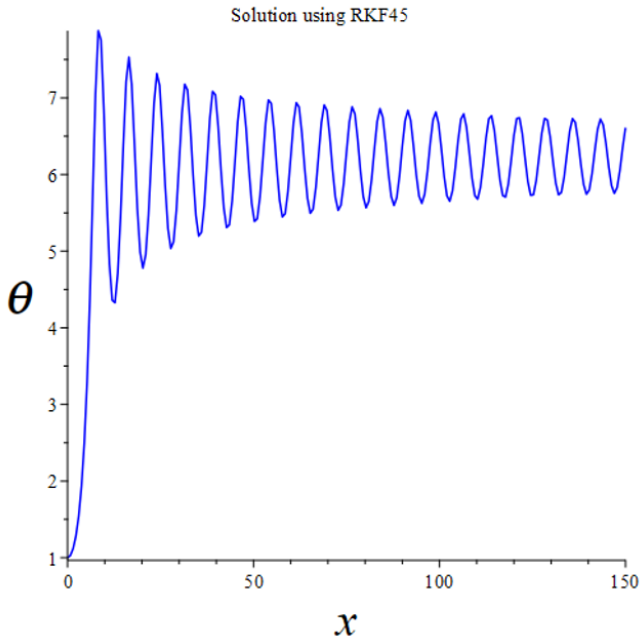

Figure 2.
RKF45 solution from Maple software**.**

From Table 1, it is observed that as the **h** is reduced from 0.1 to 0.0001, the error becomes less. Maple software was used to calculate errors and demonstration of global convergence.

Table 1.
RKF45 Global Convergence.

h	$\mathbf{E}_n$
0.1000	0.00016658335
0.0100	1.66666×10^{-7}
0.0010	1.667×10^{-10}
0.0001	1.7×10^{-13}

The second order ordinary differential equations were converted to the first order form using the following algorithm: let $\theta_1 = \theta_2 = \theta_3 = z,\ z' = z_1$ and $z'_1 = z_2$, and $\Phi_1 = \Phi_2 = \Phi_3 = s,\ s' = s_1$ and $s'_1 = s_2$. The coupled Equations 5 – 7 then take the form:

$$z_2 = -z_1 - \lambda(1+\varphi z)^m e^{z/(1+\varphi z)} + Ra((\varphi z+1)^4 - 1)$$
$$s_2 = s_1 + \lambda\epsilon_1(1+\varphi z)^m e^{z/(1+\varphi z)} \quad (10)$$

$$z_2 = -z_1 - \lambda(1+\varphi z)^m e^{z/(1+\varphi z)} - \lambda\beta_1(1+\varphi z)^m e^{\alpha_1 z/(1+\varphi z)} + Ra((\varphi z+1)^4 - 1)$$
$$s_2 = s_1 + \lambda\epsilon_1(1+\varphi z)^m e^{z/(1+\varphi z)} + \lambda\beta_1(1+\varphi z)^m e^{\alpha_1 z/(1+\varphi z)} \quad (11)$$

$$z_2 = -z_1 - \lambda(1+\varphi z)^m e^{z/(1+\varphi z)} - \lambda\beta_1(1+\varphi z)^m e^{\alpha_2 z/(1+\varphi z)} - \lambda\beta_2(1+\varphi z)^m e^{\alpha_2 z/(1+\varphi z)} + Ra((\varphi z+1)^4 - 1)$$
$$s_2 = s_1 + \lambda\epsilon_1(1+\varphi z)^m e^{z/(1+\varphi z)} + \lambda\beta_1(1+\varphi z)^m e^{\alpha_2 z/(1+\varphi z)} + \lambda\beta_2(1+\varphi z)^m e^{\alpha_2 z/(1+\varphi z)}$$
(12)

The boundary conditions take the form

$$z_1(0) = 0,\ z(1) = 0,\ s(0) = 1,\ s(1) = 1 \quad (13)$$

Maple software was used to obtain numerical solutions to study the temperature behavior and oxygen depletion caused by climate change.

3. Results and Discussion

In this section, the impact of raising the temperature in a reactive system on oxygen depletion is carried out by selecting specific parameters to study this process. The parameters to assist in this case were λ (reaction rate), and ϵ

(oxygen consumption rate). The choice of these parameters was based on their outstanding effects on temperature changes and oxygen depletion changes. The arbitrary, convenient values used were $\lambda = 0.1,\ \epsilon = 0.1$.

First, an investigation of the parameters' effects on the rate of heat exchange $\left(Nu = -\frac{d\theta}{dr}(1)\right)$ and the rate of mass transfer $\left(Sh = \frac{d\Phi}{dr}(1)\right)$ at the surface of the cylinder is represented in Tables 2 – 3. As mentioned already, for convenience, the parameters, reaction rate (λ) and oxygen consumption rate (ϵ), were considered to make the study simple to understand. Both tables indicate that an increase in the magnitude of λ reduces the rate of heat transfer at the surface of the reactive material, whereas the rate of oxygen transfer increases as the magnitude of ϵ increases. This confirms that as heat increases during the combustion of reactive materials, more oxygen is transferred into the system to accelerate the process. The tables indicate, too, that the rate of heat loss at the surface is reduced as the intensity of temperature increases. It can be observed that for the highest magnitude of the parameter, for example, $\lambda = 0.3$, in the one-step, two-step, and three-step exothermic chemical reactions, the respective values obtained from the results are -0.14790, -0.15667, and -0.16498. This is the reason why the intensity of heat is maintained at the highest points of the temperature. On the other hand, the rate of oxygen transfer at the reactive material's surface is increased to accelerate the combustion process. Again, considering the highest magnitude of $\epsilon = 0.3$ in the exothermic chemical reaction for each step, it is observed that the value of the rate of oxygen transfer is 0.01513, 0.06425, and 0.11221, in the one-step, two-step, and three-step, respectively. This scenario confirms the depletion of dissolved oxygen in the water as the temperature increases.

Table 2.
Effects of λ on Nu and Sh.

$\boldsymbol{\lambda}$	$\boldsymbol{Nu}$ **step 1**	$\boldsymbol{Sh}$ **step 1**	$\boldsymbol{Nu}$ **step 2**	$\boldsymbol{Sh}$ **step 2**	$\boldsymbol{Nu}$ **step 3**	$\boldsymbol{Sh}$ **step 3**
0.1	-0.04818	0.00506	-0.05235	0.05442	-0.05643	0.10260
0.2	-0.09746	0.01023	-0.10457	0.10770	-0.11140	0.20066
0.3	-0.14790	0.01553	-0.15667	0.15988	-0.16498	0.29455

Table 3.
Effects of ϵ on Nu and Sh.

$\boldsymbol{\epsilon}$	$\boldsymbol{Nu}$ **1-step**	$\boldsymbol{Sh}$ **1-step**	$\boldsymbol{Nu}$ **2-step**	$\boldsymbol{Sh}$ **2-step**	$\boldsymbol{Nu}$ **3-step**	$\boldsymbol{Sh}$ **3-step**
0.1	-0.04818	0.00506	-0.05235	0.05442	-0.05643	0.10260
0.2	-0.04812	0.01010	-0.05229	0.05934	-0.05636	0.10741
0.3	-0.04806	0.01513	-0.05222	0.06425	-0.05629	0.11221

Figures 3(a) – 3(c) represent the effects of the reaction rate parameter (λ) on the temperature in one-step, two-step, and three-step exothermic chemical reactions. It is observed that the temperature increases as the step of the exothermic reaction increases. This is the reason why water temperatures increase due to climate change. Elevated temperature profiles are responsible for dissolved oxygen depletion that is detrimental to the life of marine species. The values obtained, for example, $\lambda = 0.3$, show that in the one-step exothermic chemical reaction, the temperature is 0.07346, in the two-step one it is raised to 0.07623, and in the three-step reaction mechanism, it is elevated to 0.07871, as indicated in Table 4. This scenario agrees with nature since intensified heat generation in a combustion process leads to an increased temperature. On the other hand, it is observed from Figures 4(a) – 4(c) that the oxygen depletion rate increases with the rate of reaction increase. This confirms how oxygen depletion takes place faster in warm waters. Table 5 shows that, for example, at $\lambda = 0.3$, the oxygen concentration decreases as the intensity of heat goes up. In the one-step reaction mechanism, the oxygen concentration is 0.99223, in the two-step one, it is 0.92137, and it is 0.85785 in the three-step reaction process. This decline in the concentration of oxygen is experienced in water for the dissolved oxygen as the temperature is elevated to higher values. In the three-step exothermic chemical reaction process, the lowest value of the concentration confirms that at the highest temperatures during the combustion process, the depletion of oxygen is very high. Figures 5(a) – 5(c) indicate the decline in oxygen concentration as the oxygen consumption rate (ϵ) increases. The values in Table 6 confirm the behaviour of the figures. Again, taking the maximum value of $\epsilon = 0.3$, it is observed that the oxygen concentration in the one-step reaction mechanism is 0.99253, in the two-step one it is 0.96807, and in the three-step reaction mechanism the value is 0.94461. This scenario demonstrates the impact of temperature increase in water on the decrease of dissolved oxygen that is detrimental to the life of plants and animals that live in water.

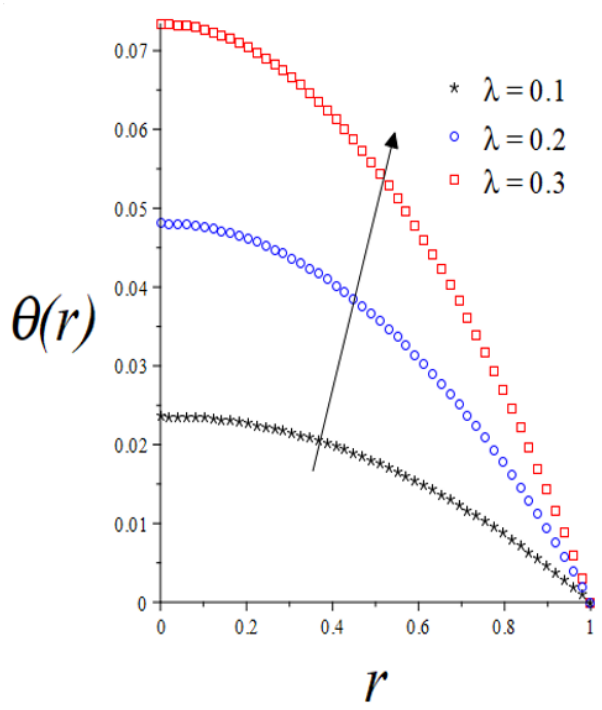

Figure 3(a).
λ effect: one-step.

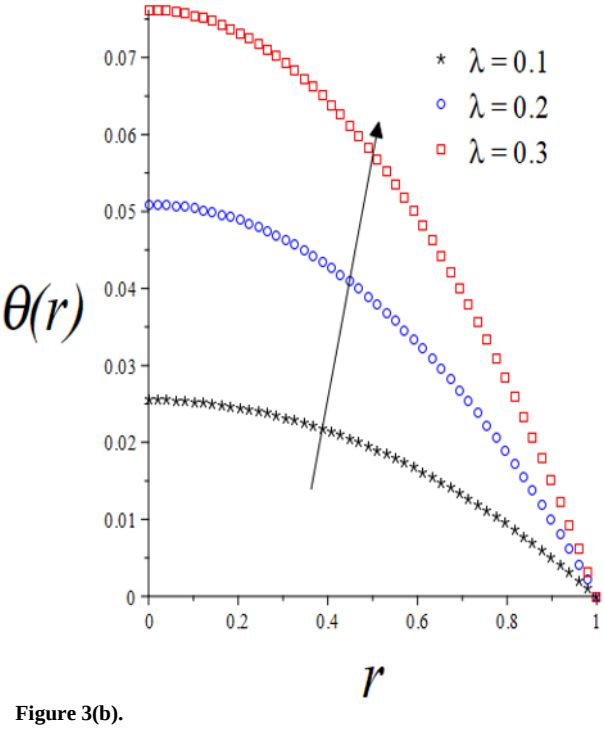

Figure 3(b).
λ effect: two-step.

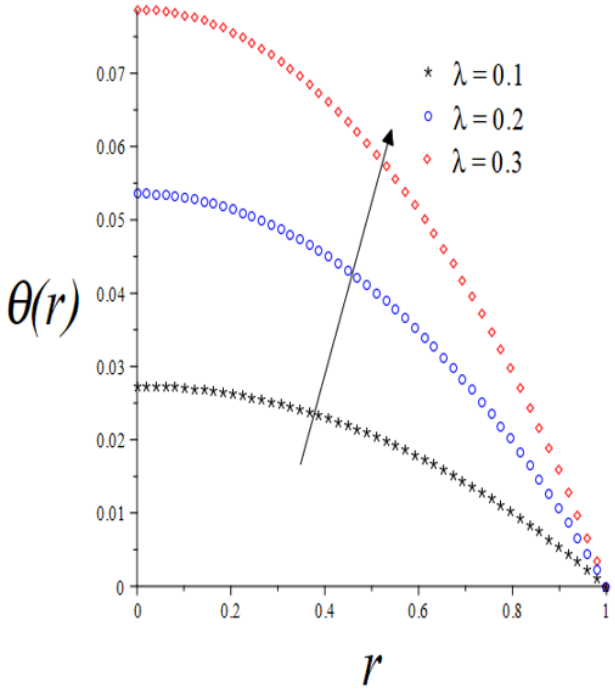

Figure 3(c).
λ effect: three-step.

Table 4.
Effects of λ on temperature.

λ	1-step	2-step	3-step
0.1	0.02365	0.02552	0.02733
0.2	0.04812	0.05093	0.05355
0.3	0.07346	0.07623	0.07871

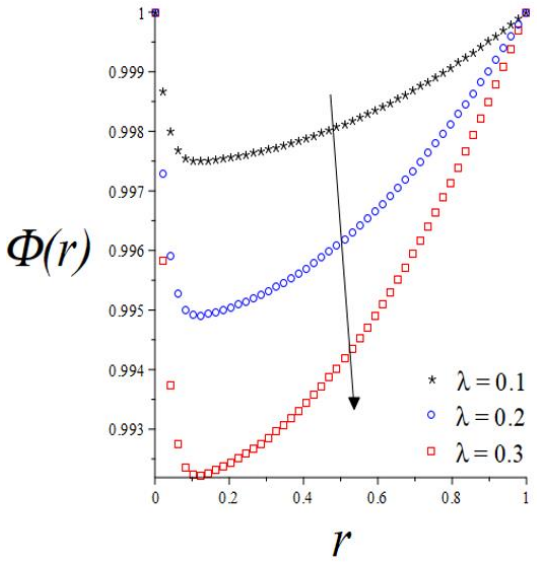

Figure 4(a).
λ effect: one-step.

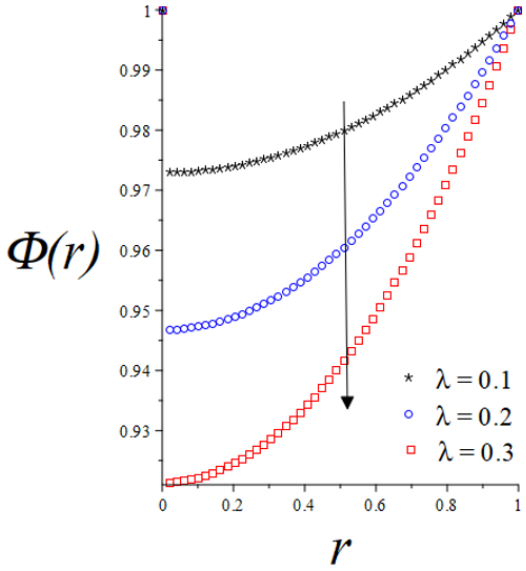

Figure 4(b).
λ effect: two-step.

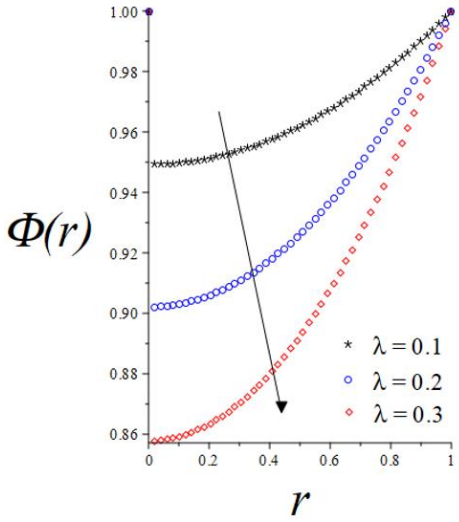

Figure 4(c).
λ effect: three-step.

Table 5.
Effects of λ on oxygen concentration.

λ	1-step	2-step	3-step
0.1	0.99755	0.97295	0.94982
0.2	0.99492	0.94675	0.90203
0.3	0.99223	0.92137	0.85785

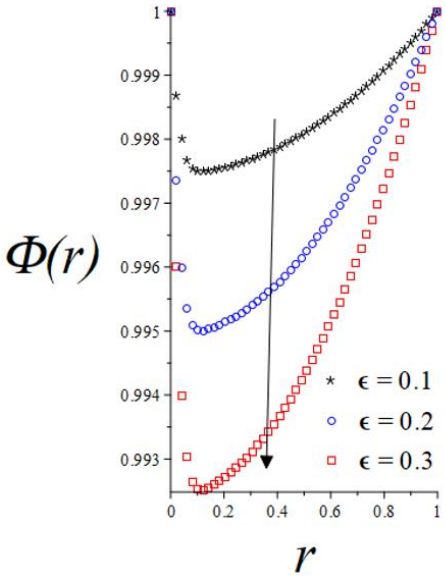

Figure 5(a).
ϵ effect: one-step.

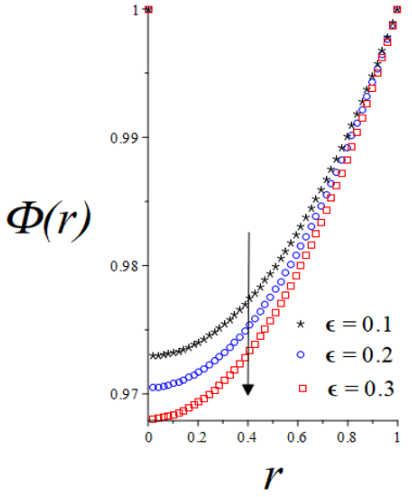

Figure 5(b).
ϵ effect: two-step.

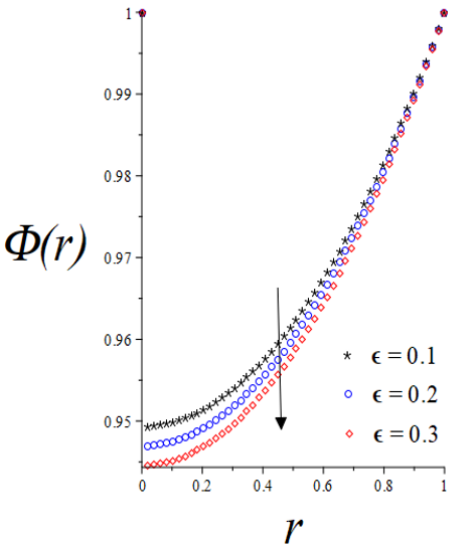

Figure 5(c).
ϵ effect: three-step.

Table 6.
Effects of ϵ on oxygen concentration.

ϵ	1-step	2-step	3-step
0.1	0.99750	0.97295	0.94932
0.2	0.99501	0.97051	0.94696
0.3	0.99253	0.96807	0.94461

4. Conclusion

The study in this investigation wanted to demonstrate the effect of temperature increase on the depletion of dissolved oxygen in water. The results showed how the relevant parameters used to demonstrate this effect were successful, using a mathematical approach that makes an understanding of the process easier for every reader. The reaction rate parameter (λ), demonstrated that an increase in the temperature of the system causes a decrease in the oxygen concentration thereof. The oxygen consumption rate parameter (ϵ), demonstrated too that the decrease in the oxygen concentration depends on the increase in the temperature of the system. The fact that the temperature in the one-step is lesser than that in the two-step and less in the three-step reaction mechanism is an indication of the increase in the intensity of heat increase in any combustion process. This study was limited to temperature changes affecting the dissolved oxygen depletion in waters but did not include the aspect of heat transfer stability due exothermic chemical reaction. Future work can include investigation of thermal stability. The importance of this study was to explain the process of heat generation and transfer in marine medium, due to climate change, that results in temperature increase and oxygen depletion that is detrimental to marine species' life. The study involved a theoretical approach which is cheaper and quicker to obtain results compared to the experimental one. This study can be extended to a rectangular or spherical domain to indicate how an increase in the temperature of a system harms the oxygen concentration.

Nomenclature:

A_1, A_2, A_3 Rate constant $[s^{-1}]$ (respective steps 1, 2, 3)
Q_1, Q_2, Q_3 Heat of reaction $[Jkg^{-1}]$ (respective steps 1, 2, 3)
E_1, E_2, E_3 Activation energy $[Jmol^{-1}]$ (respective steps 1, 2, 3)
C_1, C_2, C_3 Oxygen concentration $[moldm^{-1}]$ (respective steps 1, 2, 3)
C_w Oxygen concentration on the cylinder's surface $[moldm^{-1}]$
h Heat transfer coefficient $[Js^{-1}m^{-1}K^{-1}]$
k Thermal conductivity $[Js^{-1}m^{-1}K^{-1}]$
K Boltzmann constant $[JK^{-1}]$
l Planck number [Js]
m Numerical exponent
R Universal gas constant $[JK^{-1}mol^{-1}]$
Ra Radiation parameter (dimensionless)
T Absolute temperature of the cylinder [K]
T_W Surface temperature of the cylinder [K]
$\bar{r}$ Cylinder's radial distance [m]
r Dimensionless distance
B Biot numbers at $r = 0$ and $r = 1$ respectively
v Vibration frequency $[s^{-1}]$

Greek Symbols

$\epsilon_1, \epsilon_2, \epsilon_3$ Oxygen consumption rate parameters (respective steps 2,3)
α_1, α_2 Dimensionless energy ratio parameters (respective steps 2, 3)
β_1, β_2 Dimensionless exothermic chemical reaction parameters (respective steps 2, 3)
φ Dimensionless activation energy parameter
θ Dimensionless temperature
Φ Dimensionless concentration
μ Emissivity of the cylinder
λ Modified Frank-Kamenetskii parameter
σ Stefan-Boltzmann constant $[Wm^{-2}K^{-4}]$

References

[1] C. Mahaffey, M. Palmer, N. Greenwood, and J. Sharples, "Impacts of climate change on dissolved oxygen concentration relevant to the coastal and marine environment around the UK," *MCCIP Science Review*, vol. 2002, pp. 31-53, 2020. https://doi.org/10.14465/2020.arc02.oxy

[2] M. R. Roman and J. J. Pierson, "Interactive effects of increasing temperature and decreasing oxygen on coastal copepods," *The Biological Bulletin*, vol. 243, no. 2, pp. 171-183, 2022. https://doi.org/10.1086/722111

[3] R. M. Pilla *et al.*, "Deepwater dissolved oxygen shows little ecological memory between lake phenological seasons," *Inland Waters*, vol. 13, no. 3, pp. 327-338, 2023. https://doi.org/10.1080/20442041.2023.2265802

[4] A. Rajwa-Kuligiewicz, R. J. Bialik, and P. M. Rowinski, "Dissolved oxygen and water temperature dynamics in lowland rivers over various timescales," *Journal of Hydrology and Hydromechanics*, vol. 63, no. 4, pp. 353–363, 2015.

[5] M. R. Roman, S. B. Brandt, E. D. Houde, and J. J. Pierson, "Interactive effects of hypoxia and temperature on coastal pelagic zooplankton and fish," *Frontiers in Marine Science*, vol. 6, p. 139, 2019. https://doi.org/10.3389/fmars.2019.00139

[6] A. S. Lewis *et al.*, "Anoxia begets anoxia: A positive feedback to the deoxygenation of temperate lakes," *Global Change Biology*, vol. 30, no. 1, p. e17046, 2024. https://doi.org/10.1111/gcb.17046

[7] N. Palshin, G. Zdorovennova, T. Efremova, S. Bogdanov, A. Terzhevik, and R. Zdorovennov, "Dissolved oxygen stratification in a small lake depending on water temperature and density and wind impact," in *IOP Conference Series: Earth and Environmental Science (Vol. 937, No. 3, p. 032019). IOP Publishing*, 2021.

[8] S. F. Jane *et al.*, "Widespread deoxygenation of temperate lakes," *Nature*, vol. 594, no. 7861, pp. 66-70, 2021. https://doi.org/10.1038/s41586-021-03550-y

[9] M. Karpowicz, J. Ejsmont-Karabin, J. Kozłowska, I. Feniova, and A. R. Dzialowski, "Zooplankton community responses to oxygen stress," *Water*, vol. 12, no. 3, p. 706, 2020. https://doi.org/10.3390/w12030706

[10] M. Rajesh and S. Rehana, "Impact of climate change on river water temperature and dissolved oxygen: Indian riverine thermal regimes," *Scientific Reports*, vol. 12, p. 9222, 2022. https://doi.org/10.1038/s41598-022-12996-7

[11] S. C. Chapra, L. A. Camacho, and G. B. McBride, "Impact of global warming on dissolved oxygen and BOD assimilative capacity of the world's rivers: Modeling analysis," *Water*, vol. 13, no. 17, p. 2408, 2021. https://doi.org/10.3390/w13172408

[12] BOQU, "The impact of temperature on dissolved oxygen measurement," 2024. https://www.boquinstrument.com/a-news-the-impact-of-temperature-on-dissolved-oxygen-measurements. [Accessed 7/5/2024]

[13] A. Oschlies *et al.*, "Potential impacts of marine carbon dioxide removal on ocean oxygen," *Environmental Research Letters*, vol. 20, p. 073002, 2025. https://doi.org/10.1088/1748-9326/ade0d4

[14] R. S. Lebelo, R. K. Mahlobo, and S. O. Adesanya, "Investigating thermal stability in a two-step convective radiating cylindrical pipe," *Defect and Diffusion Forum*, vol. 408, pp. 99-107, 2021.

[15] R. S. Lebelo and S. O. Adesanya, "Oxygen depletion and thermal stability analysis in a reactive sphere of variable thermal conductivity," *Global Journal of Pure and Applied Mathematics*, vol. 13, no. 1, pp. 9-31, 2017.

[16] A. Legodi and O. D. Makinde, "A numerical study of steady state exothermic reaction in a slab with convective boundary conditions," *International Journal of the Physical Sciences*, vol. 6, no. 10, pp. 2541-2549, 2011.

[17] R. Lebelo, S. Adesanya, S. Akindeinde, and R. Mahlobo, "Investigating oxygen depletion in a two-step combustible stockpile," *Kasmera*, vol. 49, no. 1, pp. 2-10, 2021.

[18] K. I. Gasior, "Examining the influence of nondimensionalization on partial rank correlation coefficient results when modeling the epithelial mesenchymal transition," *Bulletin of Mathematical Biology*, vol. 87, no. 1, p. 15, 2025. https://doi.org/10.1007/s11538-024-01393-y

[19] J. Francisco and J. Andrés, "Mathematical modeling and analysis using nondimensionalization technique of the solidification of a splat of variable section," *Mathematics*, vol. 11, no. 14, pp. 1-16, 2022.

[20] R. S. Lebelo, R. K. Mahlobo, and S. O. Adesanya, "Reactant consumption and thermal decomposition analysis in a two-step combustible slab," *Defect and Diffusion Forum*, vol. 393, pp. 59–72, 2019.

[21] H. M. John and K. F. Kurtis, *Numerical methods using Matlab*, 4th ed. New Jersey, USA: Prentice-Hall Inc, 2004.

[22] E. Hairer, S. P. Nørsett, and G. Wanner, *Solving ordinary differential equations I: Nonstiff problems*, 2nd ed. Berlin: Springer, 1993.